







ORIGINAL RESEARCH

Possible clinical implications of the structural variations between the tympanic membrane quadrants

Firas Kassem MD^{1,2}  | Or Dagan MD³  | Ameen Biadsee MD^{1,2,4}  |
 Muhamed Masalha MD^{5,6}  | Ariela Nachmani PhD^{2,7} | Ben Nageris MD^{1,2,8} |
 Daniel J. Lee MD⁹ | Omer J. Ungar MD^{2,10}  | Ophir Handzel MD^{2,10} 

¹Department of Otolaryngology-Head and Neck Surgery, Meir Medical Center, Kfar Saba, Israel

²Sackler Faculty of Medicine, Tel Aviv University, Tel Aviv, Israel

³Department of Dermatology, Soroka Medical Center, Ben-Gurion University of the Negev, Beer-Sheva, Israel

⁴Department of Otolaryngology-Head & Neck Surgery, Western University, London, Ontario, Canada

⁵Department of Otolaryngology-Head and Neck Surgery, Emek Medical Center, Afula, Israel

⁶The Ruth and Bruce Rappaport Faculty of Medicine, the Technion Institute of Technology, Haifa, Israel

⁷Communication Disorders Faculty, Hadassah Academic College, Jerusalem, Israel

⁸Department of communication Disorders, Sackler faculty of Medicine, Tel Aviv University, Tel Aviv, Israel

⁹Department of Otolaryngology, Massachusetts Eye and Ear Infirmary, Harvard Medical School, Boston, Massachusetts, USA

¹⁰Department of Otolaryngology, Head, Neck and Maxillofacial Surgery, Tel-Aviv Sourasky Medical Center, Tel-Aviv, Israel

Correspondence

Omer J. Ungar, Division of Otolaryngology and Neurotology, Department of Otolaryngology, Head, Neck and Maxillofacial Surgery, Tel-Aviv Sourasky Medical Center, Tel-Aviv University, 6 Weizmann Street, Tel-Aviv 6423906, Israel.
 Email: ungaromer@gmail.com

Funding information

Margaret and Leo Meyer and Hans M. Hirsch Foundation

Abstract

Introduction: Retraction pockets and marginal perforations of the pars tensa of the tympanic membrane (TM) are most commonly found at superior posterior quadrant (SPQ). The patulous Eustachian tube tends to manifest in the same quadrant. Variation in the structure of the TM may explain these observations.

Material and Methods: A line defined by the manubrium was used to divide the pars tensa into anterior and posterior portions. A transverse line centered on the umbo divides the pars tensa into superior and inferior parts, resulting in four quadrants. Surface areas of each of the TM quadrants were measured in a sample of 23 human adult formalin-fixed temporal bones. The TMs were completely excised, faced medially, and placed against graph paper to maintain scale measurements, photoed, and measured.

TM thickness was measured on a different set of 20 human temporal bones (TB) preparations with normal external and middle ears. Four random loci were chosen from each pars tensa's TM quadrant. The thickness was measured using high-magnification power microscopy.

Results: The SPQ was the largest and thinnest of the four quadrants. It occupies 31% of the pars tensa area. It is 69 μm as compared to approximately 85 μm in the other quadrants. The radial lines between the umbo and the annulus are in descending order from superior posterior toward the anterior-superior radials.

Conclusion: The SPQ has the largest vibratory area and is the thinnest of the four TM quadrants. Variation in the thickness of the middle, fibrous layer accounts for the variation in the thickness of the TM. These findings may explain the tendency of pathologies related to Eustachian tube dysfunction to preferentially manifest in or originate from the SPQ.

Level of evidence: 5

KEYWORDS

Eustachian tube dysfunction, tympanic membrane area and thickness, tympanic membrane quadrants

This is an open access article under the terms of the [Creative Commons Attribution-NonCommercial-NoDerivs](https://creativecommons.org/licenses/by-nc-nd/4.0/) License, which permits use and distribution in any medium, provided the original work is properly cited, the use is non-commercial and no modifications or adaptations are made.

© 2022 The Authors. *Laryngoscope Investigative Otolaryngology* published by Wiley Periodicals LLC on behalf of The Triological Society.

1 | INTRODUCTION

The tympanic membrane (TM) is a key component of the human auditory system. It transfers sound waves from the ear canal into mechanical vibrations in the middle ear. The middle ear functions as an impedance matching apparatus and is most effective in the ambient pressure range.¹ Several physiological middle ear cleft pressure buffers exist. The most immediate mechanism for pressure buffering is the mobile nature of the TM, which is the only buffer mechanism able to control middle ear cleft volume according to Boyle's law. In the long term, the most effective mechanism for middle ear cleft pressure control is the Eustachian tube (ET). Failure of its dilatory function may result in acute and chronic otitis media, TM retraction, and cholesteatoma, all with their associated well-known morbidity and rare mortality.² Failure of its closing at rest function, known as the patulous ET (PET), can manifest in a spectrum of symptoms, at times severely affecting a patient's quality of life. Structural and mechanical changes such as TM retraction and perforation can impair sound transmission resulting in conductive hearing loss.³

The TM is divided into the pars tensa, which is anchored to the annulus, and the pars flaccida, where the annular ring is open, and the membrane is bounded by the notch of Rivinus. The pars tensa withstands negative pressure better than the pars flaccida; thus, it is less predisposed to retraction.⁴

Besides its anchoring points to the tympanic bone by annular ligament and to the malleus,^{5,6} the structure of the TM allows a considerable degree of movement, which is seen in clinical practice: medial displacement (atelectasis) as a result of ET dysfunction (ETD) induced negative middle ear cleft pressure, lateral displacement (bulging) as a result of increased middle ear cleft pressure in case of otitis media, and periodic movement as a result of a PET and pneumo-otoscopy.

Retraction pockets and marginal perforations are found most often in the pars flaccida and the superior posterior quadrant (SPQ) of the pars tensa.⁷⁻⁹ Similarly, in a PET, TM excursions synchronous with nasal breathing are most commonly seen at the SPQ. This quadrant is distanced from the protympanum and ET orifice.

The ultrastructure of the TM was extensively studied.¹⁰⁻¹⁴ Several studies found little variation between TM properties and TM quadrant,¹⁵⁻¹⁷ but others proved a significant inter-quadrantile variation of TM structure.¹⁸ In an effort to explain the high incidence of retraction pockets in the SPQ of the TM, Paço et al.¹⁰ documented the anatomic and histologic details of the SPQ. Kassem et al.⁸ measured a gradual reduction in its caliber as it approaches the SPQ.

The hypothesis of the present study is that variations in the structure of the TM are a potential cause of the frequent involvement of the SPQ in middle ear pathologies associated with ETD.

2 | MATERIAL AND METHODS

2.1 | Ethical considerations

This study was approved by the Meir Medical Center Institutional Review Board (MMC 0249-08).

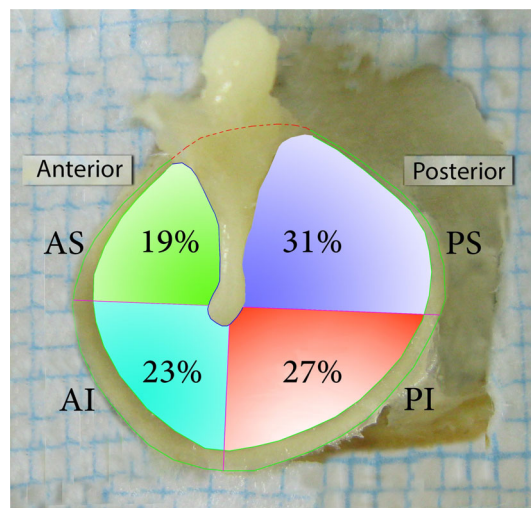


FIGURE 1 Medial view of the tympanic membrane. Purple—PS, posterior superior quadrant; Red—P; posterior inferior quadrant; Blue—AF, anterior inferior quadrant; Green—AS, anterior superior quadrant

The study comprises a histological analysis of the TM thickness performed in specimens from the TB bank at the Massachusetts Eye and Ear Infirmary (MEEI). Surface area measurements were performed at the Meir medical center in Israel.

For both parts of the study, the TM was divided into four quadrants. A perpendicular line was drawn along the axis of the manubrium. A transverse line also was drawn, crossing the perpendicular line at the midpoint of the malleolar umbo. The quadrants were distributed as SPQ, superior anterior (SAQ) inferior-posterior (IPQ), and inferior-anterior (IAQ) (Figure 1).

2.2 | MEEI part

Twenty temporal bones (TB) were randomly enrolled in the study. Included only adult's TBs (died in the 4th to 6th decade of life) of normal external and middle ears, as clinically documented and histologically analyzed. The clinical history was collected during life through enrollment in the National Institute on Deafness and Other Communication Disorders (NIDCD), National Temporal Bone, Hearing and Balance Pathology Resource Registry. Excluded all TBs with clinical or histological evidence of middle ear pathology, including myringosclerosis, TM perforation, and cholesteatoma. Additionally, all TBs of patients with epithelial or connective tissue disorders (Psoriasis, pemphigus, Marfan syndrome, etc.) were excluded.

After death, all TBs were prepared for light microscopy by fixation in formalin followed by standard processing for histologic examination, including decalcification with ethylenediamine tetra-acetic acid and celloidin embedding. All specimens were sectioned serially in the horizontal plane at a section thickness of 20 μ m. Every tenth section was stained with hematoxylin and eosin and mounted on a glass slide. The slides were examined by light microscopy.

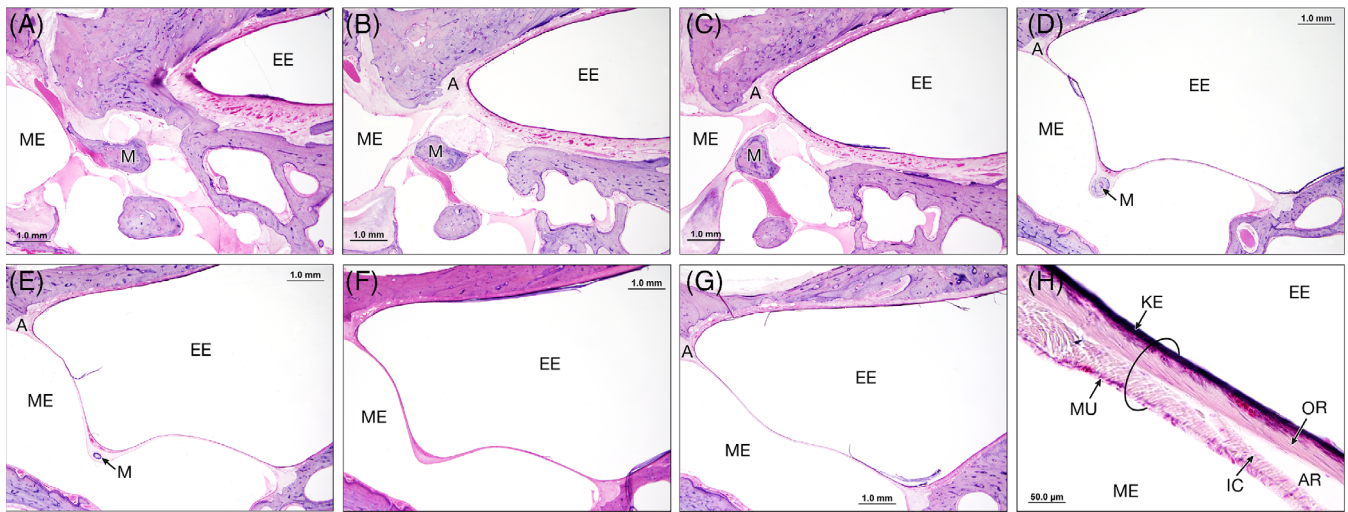


FIGURE 2 Serial horizontal section through a TB. (A) Just above the annular ligament. (B) At the level of the annular ligament. (C) One slide below (B). (D) Attachment of the malleus. (E) Inferior pole of the malleus. (F) Below the level of the malleus. (G) Artifact (desquamation) is seen. (H) High magnification of the TM. A, annulus; AR, artifact; EE, external ear; IC, inner circular; KE, keratin; M, malleus; ME, middle ear; MU, mucus; OR, outer radial

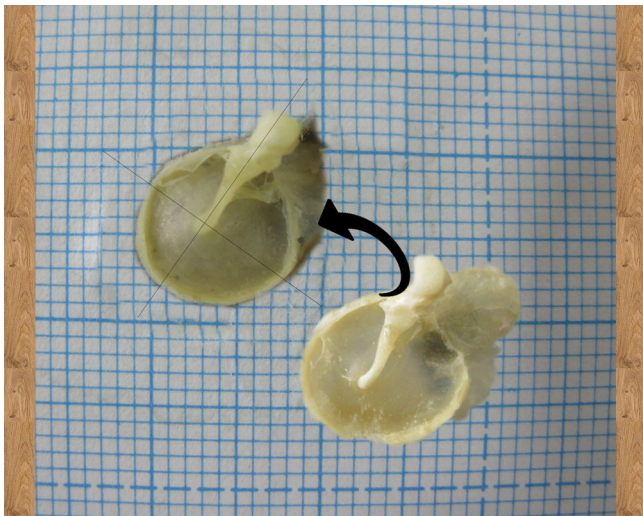


FIGURE 3 Placing the tympanic membrane and its surrounding tissues on a scaled paper in preparation for high-resolution photographing. Based on the photos and using appropriate software, radii measurements were made.

Two-dimensional graphic reconstruction of the TM was performed by identifying the annular ligament in a sequential manner. Four random loci were chosen from each pars tensa's TM quadrant. The width was measured using high-magnification power (Figure 2).

2.3 | Meir medical center part

The Meir medical center part is a sequel to the previous study by Kassem et al.⁸ The study included 23 normal human adult temporal bones from both sexes with a history of no otologic pathology or surgery.

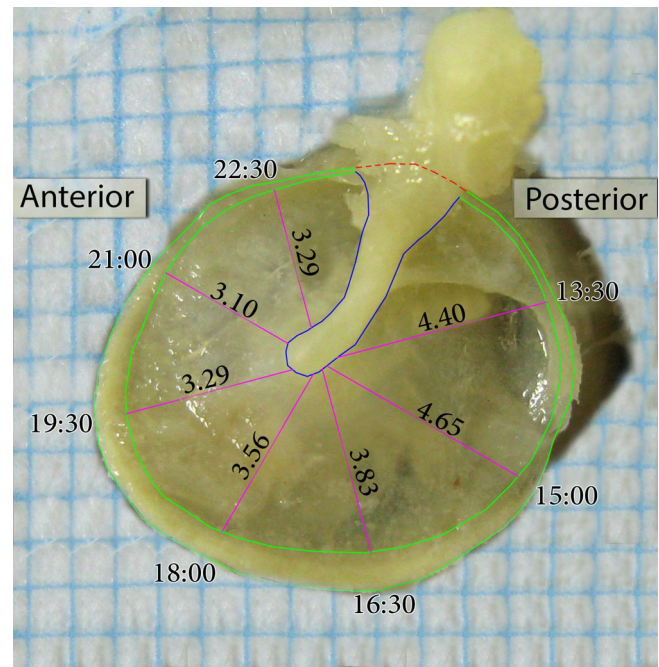


FIGURE 4 Medial view of the tympanic membrane. Pink—mean “length without the annulus” measurements at the seven axis points. Green—annular ring; Blue—borders of the manubrium

The TMs were completely extracted from the formalin-fixed temporal bones, with special care taken to preserve the annulus and the entire surface of the TM. To preserve the anatomical morphology, the eardrums included the malleus and the medial portion of the external auditory canal skin.

The TMs, including the malleus and the medial portion of the external auditory canal, were faced medially, opposite the clinician's

view through the external ear canal. The TMs were laid flat on a 1×1 -mm scale graph paper mounted on a board with a hole (Figure 3). The TMs were viewed medially and aligned with graph paper. High-resolution photographs were taken to obtain accurate images of the annulus, the surface of the TM, and the surrounding graph paper. The photographs were magnified, and the outlines of the annulus were marked by continuous lines (Figure 4). Vertical and transverse lines were drawn along the manubrium axis and the midpoint of the malleus umbo, respectively, dividing the circle-shaped boundaries of the TM into four quadrants (Figure 1). With a graph paper used as a scale, the AutoCAD 2009 drawing software was used to carry out quantitative measurements, using graph paper as a scale. The lengths measured were corrected by the 1 mm of the graph paper by ratio.

Measurements were focused on the free-moving, non-tethered area of the TM. This area was defined as the total area of the TM minus the area attached to the manubrium and the pars flaccida.

Thereafter, looking at the preparation as a clock face, measurements of the “length without annulus” (the distance of the radius in mm from the edge of the umbo to the circumference of the TM without the annulus) and “length with annulus” (the distance in mm of the radial line from the umbo to the circumference of the TM with the annulus) were taken at seven different points; 6:00 p.m. served as a midpoint, and another three points were set at each side, anteriorly and posteriorly (in clockwise and counterclockwise directions, respectively; Figure 4).

TABLE 1 Sizes of the quadrants of the human tympanic membrane

| Quadrant | Mean (mm ²) ± SD | 95% CI, range (mm ²) |
|--------------------|------------------------------|----------------------------------|
| Superior-posterior | 17.1 ± 3.2 | 15.7–18.4 |
| Inferior-posterior | 14.6 ± 2.8 | 13.4–15.8 |
| Inferior-anterior | 12.3 ± 3.2 | 10.9–13.7 |
| Superior-anterior | 10.1 ± 1.6 | 9.4–10.8 |

Note: There were significant variations in mean areas among all four quadrants. The area of the superior-posterior quadrant was significantly larger than all other quadrants ($p = .022$, $<.0001$, and $<.0001$, respectively). The difference in mean area between the inferior-anterior quadrant and the superior-anterior quadrant was close to statistically significant ($p = .055$).

TABLE 2 Comparison between different “length in” groups

| Group | Group number | Mean ± SD (mm) | (mm) | Max (mm) | Significant group correlations ^a | <i>p</i> |
|----------------------|--------------|----------------|------|----------|---|----------|
| Length in 1:30 p.m. | 1 | 4.40 ± 0.51 | 3.36 | 5.44 | 1: 3, 4, 5, 6, 7 | <.001 |
| Length in 3:00 p.m. | 2 | 4.65 ± 0.48 | 3.76 | 5.65 | 2: 3, 4, 5, 6, 7 | |
| Length in 4:30 p.m. | 3 | 3.83 ± 0.38 | 3.27 | 4.68 | 3: 1, 2, 5, 6, 7 | |
| Length in 6:00 p.m. | 4 | 3.56 ± 0.50 | 2.9 | 4.41 | 4: 1, 2, 6 | |
| Length in 7:30 p.m. | 5 | 3.29 ± 0.55 | 2.44 | 4.36 | 5: 1, 2, 3 | |
| Length in 9:00 p.m. | 6 | 3.1 ± 0.45 | 2.12 | 3.79 | 6: 1, 2, 3, 4 | |
| Length in 10:30 p.m. | 7 | 3.29 ± 0.36 | 2.58 | 3.99 | 7: 1, 2, 3 | |

Note: Comparison between different “length in” groups (“length in” mm is the distance of the radial line from the border of the umbo to the inner border of the annulus). “Length in” group refers to the specific measurement on that axis.

^aSignificant correlations of a group compared to other “length in” groups (axes).

2.4 | Statistical analysis

Categorical variables were described as frequency and percentage, and continuous variables as median and range. The continuous variables were evaluated for normal distribution using a histogram and a Q–Q plot and described as median and range. A p value $<.05$ was considered statistically significant. SPSS (IBM SPSS Statistics for Windows, version 22.0; IBM Corp.) was used for all the statistical analyses.

Data are expressed as mean, standard deviation (SD), and confidence interval. One-way analysis of variance (ANOVA) with Bonferroni correction was performed. p Values $<.05$ were considered statistically significant. The data were analyzed by using SPSS-25 (IBM).

3 | RESULTS

3.1 | MEEI part

Twenty TBs (12 males and eight females) were enrolled. Eleven right and nine left TBs were enrolled. The median age of death was 42 years (range 32–57). The median postmortem time was 11 h (range 4–19).

The TM thickness was less than 100 μm in all the loci tested, and ranged within 30 μm (62–92). The thinnest quadrant was the SPQ, with a median thickness of 69 μm ($p <.05$). The next thinnest quadrant was the SAQ, with a median thickness of 85 μm , followed by the IAQ and the IPQ, with a measured median thickness of 85.5 μm . The absolute thickness of both epithelial linings of each TM tested was not varied significantly, leaving the variation in the thickness of the middle fibrous layer to account for the variation in thickness among the tested TMs.

3.2 | Meir medical center part

Assessment of the medial surface of the TM showed that the mean area of the vibratory TM was $54.1 \pm 7.2 \text{ mm}^2$. This area was divided symmetrically by the transverse line crossing the midpoint of the

TABLE 3 Comparison between different “length out” groups

| Group | Group number | Mean \pm SD (mm) | Min (mm) | Max (mm) | Significant group correlations ^a | <i>p</i> |
|-----------------------|--------------|--------------------|----------|----------|---|----------|
| Length out 1:30 p.m. | 1 | 4.58 \pm 0.53 | 3.56 | 5.62 | 1: 2, 5, 6, 7 | <.001 |
| Length out 3:00 p.m. | 2 | 5.11 \pm 0.49 | 4.32 | 6.08 | 2: 1, 3, 4, 5, 6, 7 | |
| Length out 4:30 p.m. | 3 | 4.48 \pm 0.38 | 3.97 | 5.21 | 3: 2, 5, 6, 7 | |
| Length out 6:00 p.m. | 4 | 4.31 \pm 0.54 | 3.61 | 5.56 | 4: 2, 6, 7 | |
| Length out 7:30 p.m. | 5 | 3.69 \pm 0.57 | 2.98 | 5.28 | 5: 1, 2, 3, 7 | |
| Length out 9:00 p.m. | 6 | 3.55 \pm 0.43 | 2.68 | 4.38 | 6: 1, 2, 3, 4 | |
| Length out 10:30 p.m. | 7 | 3.50 \pm 0.35 | 2.74 | 4.14 | 7: 1, 2, 3, 4, 5 | |

Note: “Length out” (mm) is the distance of the radial line from the border of the umbo to the outer border of the annulus. “Length out” group refers to the specific measurement on the mentioned axis.

^aStatistically significant correlations of a group compared to other “length out” groups (axes).

malleolar umbo. The proportional area of the SPQ (31%) added to the proportional area of the SAQ (19%) was equal to the proportional area of the IPQ (27%) added to the IAQ (23%) (Figure 1).

The mean areas of the quadrants varied significantly. The mean area of the SPQ was significantly greater than that of the IPQ, IAQ, and SAQ (17.1 \pm 3.2 mm² vs. 14.6 \pm 2.8 mm², 12.3 \pm 3.2 mm², and 10.1 \pm 1.6 mm²; *p* = .022, .0001, and .0001, respectively). Furthermore, significant differences in the mean area of the IPQ and the IAQ and SAQ were also found (*p* = .033 and .0001, respectively). The difference in mean area between the IAQ and SAQ approached statistical significance (*p* = 0.055) Table 1.

Correlations and mean measurements of the “length without annulus” and “length with annulus” at various points along the circumference of the TM are listed in Tables 2 and 3. The maximum “length without annulus” and maximum “length with annulus” were measured at the 3:00 p.m. axis. Overall, the superior posterior radials were significantly longer than the anterior were.

4 | DISCUSSION

The TM is a pivotal component of the sound transfer mechanism. A significant portion of middle ear pathologies originates from or manifests in the SPQ of the TM. Middle ear pressure is heavily dependent on the function of the ET that opens to the SAQ of the middle ear. Hence, ETD such as those manifesting in excessive negative middle ear pressure should have an equal effect on all parts of the TM and not manifest preferentially in the SPQ. Elucidation of the variation in the structure of the TM between the superior posterior and the other quadrants may offer one possible explanation of the tendency of middle ear pathologies to manifest in the SPQ.

Our results showed that the mean area of the SPQ was significantly greater than that of all other three quadrants. Furthermore, this analysis shows that the maximum radii between the umbo and the side of the TM with and without the annulus were at the SPQ, with radials decreasing in length from the superior-posterior toward the SAQ. Hence, the SPQ has the largest vibratory area of all four TM quadrants. The SPQ is the thinnest TM quadrant, with a median

thickness of 69 μ m (*p* < 0.05) as compared to approximately 85 μ m of the other three quadrants. The absolute thickness of both epithelial linings of each pars tensa of the TM tested did not vary significantly, leaving the mesenchymal, fibrous layer to account for the variability in thickness among the compared quadrants. The biological difference between the pars tensa and pars flaccida can be found in the lamina propria. The lamina propria of the pars flaccida consists primarily of loose and unorganized connective tissue and is thicker than the pars tensa.¹⁹ The unorganized fibers in its connective tissue make the structural arrangements within the pars flaccida weaker and more likely to retract.²⁰

In agreement with our analysis, Paço et al.¹⁰ found that the SPQ has the largest area, representing 28.7% of the area of the eardrum. Nevertheless, they found a major difference in TM size in comparison with our analysis, where the TM measured 73.2 mm². This difference is because we measured the true vibratory area of the TM. Additional values of the TM area were reported between 55.4 and 85 mm².

In the current analysis, we found a gradual decrease in the difference between the “lengths without” and “lengths with annulus” while approaching the SPQ and SAQ. These results are in accordance with our previous report on the TM annulus, which showed a similar symmetrical decrease in the caliber of the annulus toward the SPQ and SAQ, creating a horseshoe-shaped appearance.⁸

Temporal bone preparation is known to cause shrinkage of the processed tissue. Both preservation with formalin and dehydration with ETOH shrink the tissue. In this study, we assume that shrinkage is evenly distributed between the four quadrants. In the radii measurements, shrinkage is limited by keeping the bone framework of the TM. It is expected to affect the absolute measurement of both thickness and radii/surface of the compared quadrant but not the relative measurements. Hence, despite shrinkage, the conclusion that the SPQ is the largest and thinnest of the four quadrants should still be valid. That being said, Kuypers et al.¹³ found no significant difference in the thickness of the same TM between fresh, fixed, and preserved conditions, making the histological measurements more clinically relevant.

The median thickness of the SPQ was 69 μ m and was close to 85 μ m for the other quadrants. The range was 30 μ m. This is in agreement with the findings of Schmidt and Hellstein.¹¹

As compared to *in vivo* measurement techniques such as Optical Coherence Tomography,²¹ our measurement may report thinner and smaller (in surface and radii) TMs. Measurement by optical coherence tomography found thickness to range from 79.6 to 97.0 μm .^{12,22,23} The anterior region was thicker than the posterior region as measured with confocal microscopy¹³ and optical coherence tomography.¹² Hand-held OCT device can offer superior ease of use.²⁴ Low coherence interferometry is another technique used for *in vivo* measurements of the thickness of the TM. Pande et al.²⁵ found that the mean and pooled standard deviation of the thickness of the different regions of the pars tensa of the TM, computed over all TMs, were found to be $137.7 \pm 56.1 \mu\text{m}$ for the posterosuperior quadrant, $93.4 \pm 23.9 \mu\text{m}$ for the posteroinferior quadrant, $76.4 \pm 20.5 \mu\text{m}$ for the anterosuperior quadrant, and $79.2 \pm 20.0 \mu\text{m}$ for the anteroinferior quadrant. Among the different quadrants of the pars tensa, the overall mean thickness of the posterosuperior quadrant was found to be higher than the other quadrants. Computing the thickness of the TM is challenging because of its cone-shaped structure. The thickness measurements at each voxel on the membrane must be taken orthogonal to the surface of the membrane.²⁴ From this aspect measurements based on post-mortem specimens and sectioned TM allow easier thickness measurements.

4.1 | Physiology

The middle ear compensates for the acoustic impedance mismatch between the ambient air and the fluid of the inner ear, mainly by the vibratory effect of the TM.¹⁴ The vibratory amplitude of the TM is dictated by a number of factors, including the annulus, ossicular chain, suspension ligaments, distribution of collagen in the lamina propria, and the different sizes of the four TM quadrants; all play a role in the stiffness of the TM.¹⁵ Khaana et al.¹⁶ found that the maximum vibration of the TM is in the SPQ and less in the anterior and inferior quadrants. These results were validated by a laser Doppler vibrometry experiment that found greater velocity and displacement in the posterior quadrants of the TM.¹⁷ It is reasonable to assume that the reduced thickness, larger vibratory area of this quadrant, and longer radials contribute to this vibration pattern.

4.2 | Pathological implications

Retraction pockets may lead to chronic infection and inflammation of the middle ear, including marginal perforation and cholesteatoma, with or without ossicular chain destruction.²⁶ Retraction pockets are most commonly found in the pars flaccida and the SPQ of the pars tensa.^{10,18,26} Many theories have been proposed to explain the prevalence of retraction pockets and marginal perforations in the SPQ. Bhide et al.⁷ suggested that this quadrant is most vulnerable, due to its wide-angle insertion into the bony canal, which bares it to the thrust effect of the air column in the external auditory canal. Kassem et al.⁸ found that the tympanic mean maximum caliber annulus was

measured at the manubrium axis. From that point, the annulus gradually thinned out in both directions, until it reached about 15% of its maximum caliber at the SPQ and SAQ. It was also found that the annular ligament was absent in the pars flaccida region. These findings are in accordance with the high incidence of retraction pockets in the pars flaccida and the SPQ.⁸ Jackler et al.²⁷ suggested that retraction pockets are more common in the SPQ in comparison to the others, due to different epithelial migration patterns in the posterior part of the TM. As opposed to anterior tympanic traction, which was only radial, superior posterior traction was dominant in the posterior portion.²⁷ In the analysis by Paço et al.,¹⁰ the SPQ was characterized by the absence of circular fibers of the lamina propria, which only had a layer of radial fibers. Furthermore, the anterior malleolar ligament was suggested to protect the SAQ.¹⁰ In our analysis, we found that the largest area and longest radials of the TM were in this quadrant. It is known that the greater the length of a thread, the more vulnerable is its center.²⁸ The same principle can be applied to the longer radials of the SPQ, which provides another explanation for the decreased ability of this area to withstand negative pressure.

The analysis provided here shows that the SPQ is the largest and that the IPQ was larger than the anterior quadrants. Mills et al.⁹ surveyed 93 ears with retraction pockets and summarized that 56% involved both the superior-posterior and inferior-posterior quadrants, 28% involved only the superior-posterior and 9% involved the entire TM. Furthermore, Cassano et al.²⁹ mapped the distribution of retraction pockets in 22 patients and found the following prevalence: superior-posterior, inferior-posterior, and thereafter, the anterior quadrants, which had similar numbers. Although reports about quadrant distribution of retraction pockets are few in number, they might reflect a connection between quadrant sizes and the location of retraction pockets.

The study has a number of limitations. Surface area measurements of the TM were a two-dimensional projection of a three-dimensional conical structure. This is a simplification of the actual radii and surface sizes of the TM quadrants. The transposition should have a limited influence on the comparison between the radii of the four-quadrant as it affects all of them, as the approximation should have a reasonably similar influence on the measurements of each of the four quadrants. The dynamic properties of the TM were not measured. A larger surface and thinner TM is not necessarily more compliant and less resistant to pressure changes TM, although this assumption is a logical one. The TM composition and thickness change with age. The TM becomes less vascular, less cellular, more rigid, and less elastic.³⁰ These changes may influence the tendency of the TM to respond to a change in middle ear pressure and have not been accounted for in our study. According to the process of the human temporal bone for histological preparation, the inferior most 2 mm of the middle ear is often removed; hence, the lowest part of the TM is not represented in the area samples for thickness measurements. Surface area measurements were made disregarding the natural convexity of the TM between the manubrium and annulus. As all four quadrants are convex the actual impact of this approximation should be limited.

5 | CONCLUSION

The SPQ has the largest vibratory area and is the thinnest of the four TM quadrants. Variation in the thickness of the middle, fibrous layer accounts for the variation in the thickness of the TM. These findings may explain the tendency of pathologies to preferentially manifest in or originate from the SPQ.

ACKNOWLEDGMENTS

This study has been supported by the Margaret and Leo Meyer and Hans M. Hirsch Foundation (Daniel J. Lee and Ophir Handzel). The authors express their most profound appreciation for tissue donors. They would like to thank Faye Schreiber for editing the manuscript and Barak Levi for physicist consulting.

CONFLICT OF INTEREST

The authors declare no conflict of interest.

DATA AVAILABILITY STATEMENT

Data are available upon a written request to the corresponding author.

ORCID

Firas Kassem  <https://orcid.org/0000-0003-3715-1120>

Or Dagan  <https://orcid.org/0000-0003-2425-5414>

Ameen Biadsee  <https://orcid.org/0000-0002-3768-6216>

Muhamed Masalha  <https://orcid.org/0000-0001-7344-4962>

Omer J. Ungar  <https://orcid.org/0000-0002-5904-1291>

Ophir Handzel  <https://orcid.org/0000-0002-6905-3034>

REFERENCES

1. Terkildsen KNUT, Thomsen KA. The influence of pressure variations on the impedance of the human ear drum: a method for objective determination of the middle-ear pressure. *J Laryngol Otol.* 1959;73(7):409-418.
2. Bluestone MB, ed. *Eustachian Tube: Structure, Function, Role in Otitis Media.* BC Decker; 2005.
3. Huang G, Daphalapurkar NP, Gan RZ, Lu H. A method for measuring linearly viscoelastic properties of human tympanic membrane using nanoindentation. *J Biomech Eng.* 2008;130(1):014501.
4. Knutsson J, Bagger-Sjöbäck D, von Unge M. Distribution of different collagen types in the rat's tympanic membrane and its suspending structures. *Otol Neurotol.* 2007;28(4):486-491.
5. Sadé J. Atelectatic tympanic membrane: histologic study. *Ann Otol, Rhinol Laryngol.* 1993;102(9):712-716.
6. Von Békésy G, Wever EG. *Experiments in Hearing.* Vol 8. McGraw-Hill; 1960.
7. Bhide A. Etiology of the retraction pocket in the posterosuperior quadrant of the eardrum. *Arch Otolaryngol.* 1977;103(12):707-711.
8. Kassem F, Ophir D, Bernheim J, Berger G. Morphology of the human tympanic membrane annulus. *Otolaryngol-Head Neck Surg.* 2009;3(141):P86.
9. Mills RP. Management of retraction pockets of the pars tensa. *J Laryngol Otol.* 1991;105(7):525-528.
10. Paço J, Branco C, Estibeiro H, Oliveira e Carmo D. The posterosuperior quadrant of the tympanic membrane. *Otolaryngol-Head Neck Surg.* 2009;140(6):884-888.
11. Schmidt SH, Hellström S. Tympanic-membrane structure—new views. *ORL J Otorhinolaryngol Relat Spec.* 1991;53(1):32-36.
12. Van der Jeught S, Dirckx JJ, Aerts JR, Bradu A, Podoleanu AG, Buytaert JA. Full-field thickness distribution of human tympanic membrane obtained with optical coherence tomography. *J Assoc Res Otolaryngol.* 2013;14(4):483-494.
13. Kuypers LC, Dirckx JJ, Decraemer WF, Timmermans JP. Thickness of the gerbil tympanic membrane measured with confocal microscopy. *Hear Res.* 2005;209(1-2):42-52.
14. Fay J, Puria S, Decraemer WF, Steele C. Three approaches for estimating the elastic modulus of the tympanic membrane. *J Biomech.* 2005;38(9):1807-1815.
15. O'Connor KN, Tam M, Blevins NH, Puria S. Tympanic membrane collagen fibers: a key to high-frequency sound conduction. *Laryngoscope.* 2008;118(3):483-490.
16. Khanna SM, Tonndorf J. Tympanic membrane vibrations in cats studied by time-averaged holography. *J Acoust Soc Am.* 1972;51(6B):1904-1920.
17. Szymański M, Rusinek R, Zadrożniak M, Warmiński J, Morshed K. Drgania błony bębenkowej oceniane Dopplerowskim wibrometrem laserowym. *Otolaryngol Pol.* 2009;63(2):182-185.
18. Sadé J, Shatz A. Cholesteatoma in children. *J Laryngol Otol.* 1988;102(11):1003-1006.
19. Bayoumy AB, Veugen CC, van der Veen EL, Bok JWM, de Ru JA, Thomeer HG. Management of tympanic membrane retractions: a systematic review. *Eur Arch Otorhinolaryngol.* 2022;279:723-737.
20. Lim DJ. Structure and function of the tympanic membrane: a review. *Acta Otorhinolaryngol Belg.* 1995;49(2):101-115.
21. Tan HEI, Santa Maria PL, Wijesinghe P, et al. Optical coherence tomography of the tympanic membrane and middle ear: a review. *Otolaryngol-Head Neck Surg.* 2018;159(3):424-438.
22. Djalilian HR, Ridgway J, Majestic Tam AS, Chen Z, Wong BJ. Imaging the human tympanic membrane using optical coherence tomography in vivo. *Otol Neurotol.* 2008;29(8):1091.
23. Hubler Z, Shemonski ND, Shelton RL, Monroy GL, Nolan RM, Boppart SA. Real-time automated thickness measurement of the in vivo human tympanic membrane using optical coherence tomography. *Quant Imaging Med Surg.* 2015;5(1):69.
24. Lui CG, Kim W, Dewey JB, et al. In vivo functional imaging of the human middle ear with a hand-held optical coherence tomography device. *Biomed Opt Express.* 2021;12(8):5196-5213.
25. Pande P, Shelton RL, Monroy GL, Nolan RM, Boppart SA. A mosaic-like approach for in vivo thickness mapping of the human tympanic membrane using low coherence interferometry. *J Assoc Res Otolaryngol.* 2016;17(5):403-416.
26. Sadé J, Avraham S, Brown M. Atelectasis, retraction pockets and cholesteatoma. *Acta Otolaryngol.* 1981;92(1-6):501-512.
27. Jackler RK, Santa Maria PL, Varsak YK, Nguyen A, Blevins NH. A new theory on the pathogenesis of acquired cholesteatoma: mucosal traction. *Laryngoscope.* 2015;125:S1-S14.
28. Chen WF, Han DJ. *Plasticity for Structural Engineers (J Ross Publishing).* Blurb, Incorporated; 2007.
29. Cassano M, Cassano P. Retraction pockets of pars tensa in pediatric patients: clinical evolution and treatment. *Int J Pediatr Otorhinolaryngol.* 2010;74(2):178-182.
30. Ruah CB, Schachern PA, Zelterman D, Paparella MM, Yoon TH. Age-related morphologic changes in the human tympanic membrane: a light and electron microscopic study. *Arch Otolaryngol-Head Neck Surg.* 1991;117(6):627-634.

How to cite this article: Kassem F, Dagan O, Biadsee A, et al. Possible clinical implications of the structural variations between the tympanic membrane quadrants. *Laryngoscope Investigative Otolaryngology.* 2022;7(4):1164-1170. doi:10.1002/lio2.861